Roles of waste carbon fibers on the efficiency of multiple induction heating healing behavior in asphalt mixture for sustainable infrastructure

Ye, Xiangqian; Xiao, Zhenyong; He, Chuang; Li, Wenyu; Lin, Peng; Meng, Yuanyuan; Hu, Chichun

DOI
10.1016/j.jclepro.2023.138694

Publication date
2023

Document Version
Final published version

Published in
Journal of Cleaner Production

Journal of Cleaner Production 423 (2023) 138694

Contents lists available at ScienceDirect

Journal of Cleaner Production

journal homepage: www.elsevier.com/locate/jclepro

Roles of waste carbon fibers on the efficiency of multiple induction heating healing behavior in asphalt mixture for sustainable infrastructure

Xiangqian Ye [a], Zhenyong Xiao [b], Chuang He [c], Wenyu Li [a], Peng Lin [d], Yuanyuan Meng [a], Chichun Hu [a,*]

[a] College of Civil Engineering & Transportation, South China University of Technology, Guangzhou, Guangdong, 510640, China
[b] Guangzhou Communications Investment Group Co. LTD, Guangzhou, Guangdong, 510330, China
[c] Guangzhou Expressway Management Co. LTD, Guangzhou, Guangdong, 510330, China
[d] Section of Pavement Engineering, Department of Engineering Structures, Faculty of Civil Engineering and Geosciences, Delft University of Technology, Netherlands

ARTICLE INFO

Handling Editor: Zhen Leng

Keywords:
Waste carbon fibers (WCFs)
Induction heating efficiency
Multiple healing behavior
Asphalt mixture
Sustainable infrastructure
Resource reutilization

ABSTRACT

This study systematically investigated the potential of waste carbon fibers (WCFs) as a sustainable solution in enhancing the multiple induction heating healing of asphalt mixture, thereby tackling two major concerns: the environmental impact of WCFs and the durability of asphalt pavement. Firstly, four groups of asphalt binder samples with different WCFs contents were prepared. The viscosity and workability of WCFs modified asphalt binder were analyzed. Next, asphalt mixture containing 2% steel fibers was prepared at the optimal WCFs content, while control groups without WCFs were prepared with 2% and 4% steel fibers content. A comprehensive study was conducted on the induction heating rate, effective heating depth and surface temperature cooling rules of the asphalt mixture. Finally, by conducting multiple "fracture-healing" tests, the influence of WCFs on the healing efficiency of asphalt mixture was analyzed. The results revealed that WCFs increased the viscosity of the virgin asphalt, but excessive WCFs content hindered the workability. The optimal WCFs content was determined to be 1% (by weight of asphalt binder). WCFs enhanced the thermal conductivity of the asphalt mixture, accelerating heating and improving vertical heat transfer while reducing surface temperature decline. During multiple "fracture -healing" processes, the inclusion of WCFs enhanced the mechanical strength of the asphalt mixture, improved its healing efficiency, and increased the number of healings. Even after five cycles, the specimen with the most damage still showed a fracture energy recovery rate (FERR) of over 30%. In conclusion, WCFs significantly enhanced the multiple induction heating healing efficiency of the asphalt mixture.

1. Introduction

Asphalt mixture is a widely used material in highway and urban road construction due to its excellent performance in terms of traffic safety, driving stability, and fast traffic time (Meng et al., 2022; Qin et al., 2021; Wan et al., 2021). However, asphalt pavement is prone to develop cracks over time due to temperature fluctuations (Norouzi and Richard Kim, 2017; Souza and Castro, 2012), traffic load (Loizos and Karlaftis, 2005; Wang and Zhong, 2019), moisture infiltration (Khodaii et al., 2014; Mirhosseini et al., 2016), and construction quality (Schuster et al., 2023), which not only reduces the service life of the pavement but also affects the pavement structure and vehicle traffic safety (Li et al., 2019; Zhang et al., 2019). After asphalt road cracking occurs, it is necessary to take appropriate maintenance measures to repair the cracks and prevent the occurrence of other pavement diseases. Given the substantial consumption and increasing demand for natural resources in asphalt pavement maintenance, numerous endeavors have been undertaken to create sustainable pavements, which have hastened the implementation of clean and efficient maintenance technologies in the paving industry (Ayar et al., 2016; Gonzalez-Torre and Norambuena-Contreras, 2020). In recent years, self-healing asphalt mixture has emerged as a promising solution to mitigate these issues (Anupam et al., 2022).

Currently, there are three main categories of accelerated self-healing methods for asphalt mixture: microcapsule healing, microwave heating, and induction heating (Liang et al., 2021; Sun et al., 2018; Xu et al., 2018). Notably, induction heating outperforms microwave heating in uniformity, efficiency, and avoidance of excessive heating. This approach also mitigates environmental and health concerns linked to

* Corresponding author.
E-mail address: cthu@scut.edu.cn (C. Hu).

https://doi.org/10.1016/j.jclepro.2023.138694
Received 31 May 2023; Received in revised form 14 August 2023; Accepted 3 September 2023
Available online 5 September 2023

intense microwave radiation. Furthermore, it simplifies the process by eliminating microcapsules and allows for repetitive healing. In contrast, microcapsule healing offers singular healing (Ayar et al., 2016; Garcia et al., 2020; Karimi et al., 2021; Liu et al., 2019). Asphalt mixture self-healing through induction heating has been extensively studied and validated in laboratory settings, as evidenced by references (Garcia et al., 2011, 2020; Gómez-Meijide et al., 2018; Liu et al., 2011, 2013). The composition of asphalt, including dense stone mastic asphalt and porous asphalt, has been optimized for induction heating, taking into account the type and quantity of electrically conductive particles (Ajam et al., 2018; Gómez-Meijide et al., 2016; Vila-Cortavitarte et al., 2018). Among the commonly used conductive particles, steel fibers have shown significant benefits in enhancing self-healing capability of asphalt mixture when used within the recommended range of 1%–4% by mass (Ajam et al., 2018).

However, most of the current research has only focused on the single-time healing of asphalt mixture under induction heating. In practical applications, it is necessary to achieve healing of asphalt mixture at different stages. "Multiple heating healing" refers to the process of subjecting asphalt mixture to three or more "fracture-healing" cycles, wherein after each fracture, the asphalt mixture is self-healed through induction heating. This method can effectively assess the recovery of mechanical properties of asphalt mixture after multiple "fracture-healing" cycles. (Amani et al., 2020).

One innovative approach to achieve multiple induction heating healing in asphalt mixture is the use of waste carbon fibers in combination with induction heating. Waste carbon fibers, byproducts generated in various industries such as aerospace, automotive, and wind energy, are typically discarded, contributing to environmental challenges (Cheng et al., 2022; Tapper et al., 2020). While conventional carbon fibers have been extensively studied for their role in reinforcing and self-healing asphalt mixtures (Mawat and Ismael, 2020; Slebi-Acevedo et al., 2019; Wang et al., 2016; Yang et al., 2023), the distinctive attributes of WCFs, arising from their diverse sources, sizes, and arrangements (Akbar and Liew, 2020; Li et al., 2023), set them apart. The thermal conductivity of waste carbon fiber is excellent, but the heating speed under electromagnetic induction is relatively slow. To harness their potential within asphalt mixtures, they must be combined with steel fibers to establish a conductive network. This network facilitates the efficient absorption of electromagnetic energy during the induction heating process. Consequently, the heating process is accelerated, enabling rapid localized heating of the asphalt mixture around microcracks. The energy absorbed plays a crucial role in softening the asphalt, reducing viscosity, improving flowability, and ultimately leading to a self-healing phenomenon. Despite these promising attributes, the precise extent and mechanisms through which WCFs influence the effectiveness of multiple heating healing in asphalt mixture remain unclear.

This study explored roles of WCFs on the efficiency of multiple induction heating healing behavior in asphalt mixture. Research was conducted to investigate the variation patterns of asphalt viscosity and workability with different levels of WCFs content. The optimal dosage of WCFs in asphalt was determined. Subsequently, asphalt mixture containing steel fibers was prepared at the optimal dosage of WCFs, and two control groups were set up to analyze the effect of WCFs on the induction heating performance of asphalt mixture. Finally, the changes in peak load and healing rate of asphalt mixture under multiple "fracture-healing" cycles were quantitatively analyzed by a semi-circular bending test (SCB). This research provides new avenues and theoretical support for improving the self-healing properties of asphalt mixture while addressing the challenges of waste management.

2. Materials and test methods

2.1. Raw materials

The binder chosen for this research was 70# virgin asphalt, the characteristics of which are detailed in Table 1. The aggregates employed in the study were sourced from Guangzhou, China, their essential physical parameters being outlined in Table 2. Steel fibers were also integrated into the asphalt mixture; these fibers exhibited an average length of 2.5 mm and a diameter of 65 μm. Depending on the experimental setup, their contribution to the mass of the asphalt mixture varied between 2% and 4%. A critical component of our study, Waste Carbon Fibers (WCFs), were procured from Shenzhen, China. These fibers were residual materials from the carbon fiber spinning process, along with offcuts produced during the cutting and shaping operations associated with carbon fibers. The technical properties and specifications of the WCFs are provided in Table 3.

2.2. Preparation of WCFs modified asphalt and asphalt mixture

2.2.1. Preparation of WCFs modified asphalt

In order to achieve a homogeneous dispersion of waste carbon fibers within the asphalt mixture, a procedure was implemented whereby the WCFs were incorporated into the virgin asphalt to synthesize WCF-modified asphalt (WCFMA). The detailed steps are outlined as follows.

The preparation of WCFMA involves a sequence of distinct stages. Initially, the WCFs were subjected to a drying process at 110 °C for an hour, ensuring removal of any residual moisture. Subsequently, the virgin asphalt was heated to a temperature of 165 °C. To circumvent clumping of the WCFs within the asphalt, they were gradually incorporated into the heated asphalt over a span of 10 min. Following the addition of WCFs, a high-speed shear operating at 4500 r/min was employed to facilitate swift and uniform distribution of WCFs in the heated asphalt, maintained at 165 °C ± 5 °C for 30 min. Post shearing, the asphalt mix was transferred to an oven set at 130 °C and was left undisturbed for 2 h, or until no visible bubbles surface from the asphalt mix. To experiment with the impact of WCFs content on the asphalt properties, three different concentrations of WCFs were utilized, namely 1%, 2%, and 3% by weight of the virgin asphalt. Table 4 provides the identification details of each WCF-modified asphalt (WCFMA) mixture.

2.2.2. Preparation of asphalt mixture

Fig. 1 displays the aggregate gradation of the asphalt mixture utilized in this study. Asphalt mixture incorporating 2% steel fiber (by weight of the asphalt mixture) was prepared at the optimal WCFs dosage. Two control groups were created using Pen70 asphalt: one set of asphalt mixture was prepared with 2%wt steel fiber, and another with 4%wt steel fiber. Table 5 details the identifications of asphalt mixture.

Various test methods can be employed to assess the self-healing performance of asphalt mixture, including three-point bending, four-point bending fatigue, indirect tensile, direct tensile, and semi-circular bending (SCB) tests. Among these, the SCB test stands out due to its simplicity and flexibility in sample acquisition through methods like Marshall, rotary compaction, and core-drilling sampling. Moreover, the SCB test yields results that closely correlate with actual road performance, making it the preferred choice for evaluating the healing capability of asphalt mixture (Badroodi et al., 2020; Liu et al., 2022; Zhu

Table 1
Physical properties of 70# virgin asphalt.

Physical properties	Test results	Test methods (JTG E20-2011)
Penetration (25 °C, 100 g, 5 s; 0.1 mm)	66	T0604
Softening point (°C)	49	T0606
Ductility (15 °C, 5 cm/min; cm)	>100	T0605
Viscosity (135 °C; Pa·s)	0.526	T0625
RTFOT		
Mass loss (%)	0.1	T0608
Residual penetration (%)	63	T0604
Ductility (15 °C, 5 cm/min; cm)	22	T0605

Table 2
Basic physical performance of aggregates.

Aggregate type	properties	Test results	Test method (JTG E42-2005)
Coarse aggregate	Aggregate crushing value (%)	10.2	T0316
	Los Angeles wear value (%)	11.4	T0317
	Apparent relative density	2.951	T0304
	Water Absorption (%)	0.5	T0308
	Pin content (%)	4.9	T0312
	Soft soil content (%)	0.4	T0320
	Less than 0.075 mm particle content (%)	0.1	T0310
Fine aggregate	Apparent relative density	2.882	T0328
	Mud content (%)	1.4	T0333
	Sand equivalent (%)	75	T0334

Table 3
Technical specifications of WCFs.

Technical specifications	Test results
Tensile strength (GPa)	1.68
Tensile modulus (GPa)	752
Diameter (μm)	10
Average fiber length (mm)	<3
Electrical resistivity (Ω·m)	10^{-3}

Table 4
Identifications of asphalt binders.

Binder types	Identifications
Virgin asphalt	Pen70
WCFMA with 1 wt% WCFs content	WCFMA1
WCFMA with 2 wt% WCFs content	WCFMA2
WCFMA with 3 wt% WCFs content	WCFMA3

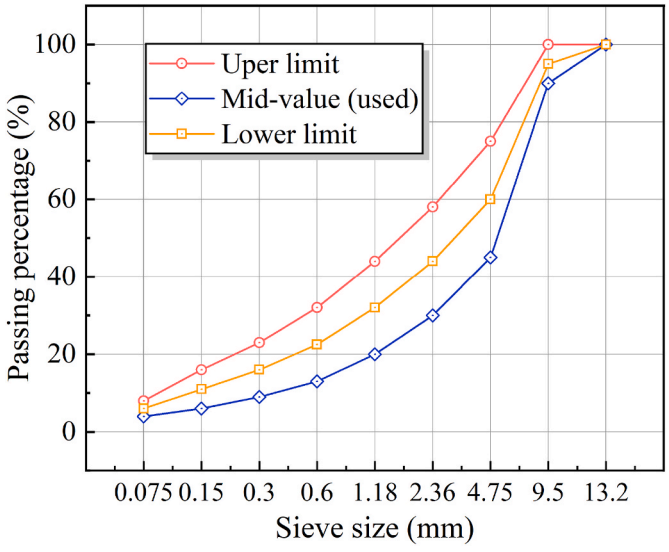

Fig. 1. Aggregate gradation used for asphalt mixture.

Table 5
Identifications of asphalt mixture.

Asphalt mixture	Identifications
WCFMA1+2%wt steel fibers	W2
Pen70 + 2%wt steel fibers	P2
Pen70 + 4%wt steel fibers	P4

et al., 2020).

In this study, testing was conducted using SCB samples with a thickness of 50 mm. The preparation process is illustrated in Fig. 2. During the forming process, a double-sided saw needed to be used to symmetrically cut the specimens formed by Superpave Gyratory Compactor (SGC). SCB specimens of 50 mm thickness were prepared, with predetermined notch depths of 10 mm, 15 mm, and 20 mm. After cutting, the samples were left at room temperature for over 24 h to ensure complete drying. Similar procedures have been employed in previous research studies as well (Fakhri et al., 2020; Liu et al., 2022).

2.3. Viscosity and workability characterization of WCFMA

Rotational viscosity offers insights into flow characteristics, temperature sensitivity, and workability—critical aspects during the induction heating healing process. The interplay between flow characteristics, temperature susceptibility, and the healing efficiency is substantial (Cao et al., 2018). To determine the optimal dosage of WCFs, measurements of rotational viscosity were conducted on Pen70 and WCFMA at five different temperatures (120 °C, 135 °C, 150 °C, 165 °C, 180 °C) using a Brookfield viscometer (DVIII).

2.4. Heating characteristics of asphalt mixture

As shown in Fig. 3, this study utilized the DDCGP-60 ultra-high frequency induction heating equipment produced by Shenzhen Dongda Co., Ltd. The output frequency of the equipment is 285 kHz, and the output power is 9.2 kW. The induction heating equipment consists of a cooling water tank, an ultra-high frequency electromagnetic induction heating equipment body, and a 15cm × 15 cm coil. The induction heating equipment generates an inductive magnetic field to heat the conductive fillers inside the asphalt mixture. Additionally, to accurately monitor the temperature changes of asphalt mixture, the DS-2TPH13-3AVF handheld thermal imager was used to collect temperature data throughout the entire heating process. The collected data was then imported into the HIKMICRO Analyzer thermal imaging analysis software, which was compatible with the thermal imager. This software allows for the analysis of temperature data for each point in the image as well as the temperature conditions within defined regions (such as maximum temperature, minimum temperature, average temperature, etc.). The induction heating rate, vertical temperature transfer, cooling patterns of asphalt mixture were investigated.

2.4.1. Induction heating rate

During the induction heating process, the room temperature was maintained at 25 ± 1 °C. A 15 × 15 cm square copper coil was used, with an induction heating distance of 10 mm. In order to enhance the vertical heat transfer inside the asphalt mixture and avoid overheating of the surface temperature, a heating mode of 3 s on and 1 s off was adopted. Real-time temperature was recorded.

As shown in Fig. 4, the average temperature within a depth range of 5 mm from the upper surface was used as the average temperature of the upper surface, and the temperature was recorded once per second. Heating was stopped when the average temperature of the upper surface reached 110 °C.

2.4.2. Effective heating depth

As shown in Fig. 4, based on the results of previous experiments, a temperature of 50 °C was taken as the effective healing temperature of asphalt mixture. After heating stopped, the depth corresponding to 50 °C in the vertical direction was read every minute.

2.4.3. Cooling rate

Fig. 4 explains the test method for the cooling rate of asphalt mixture. After the heating ended, the average surface temperature of the asphalt mixture was recorded every minute. The test was halted when

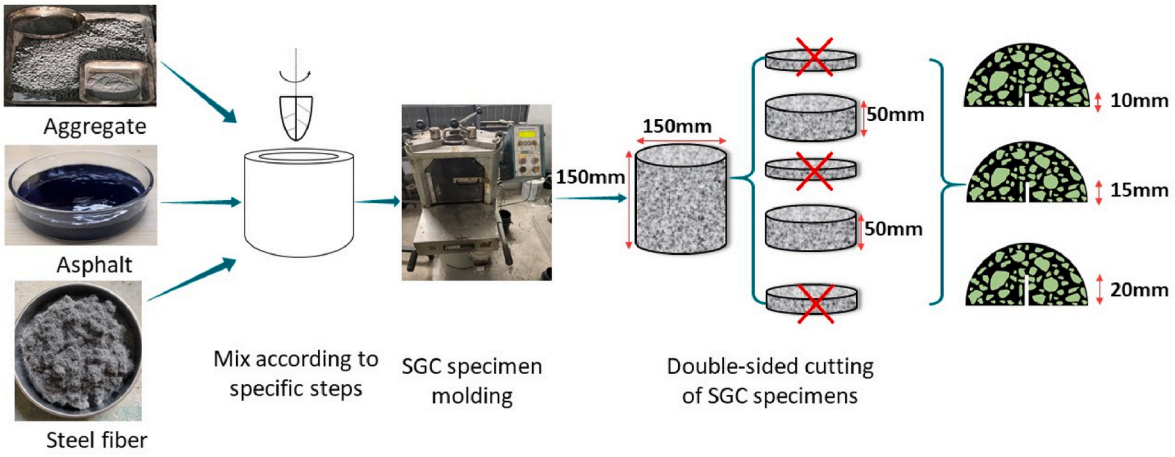

Fig. 2. SCB specimens molding and cutting process.

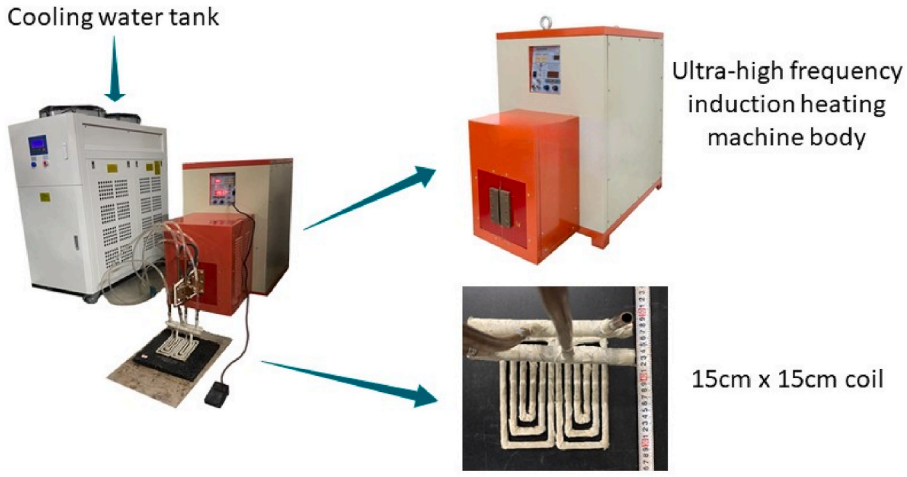

Fig. 3. Electromagnetic induction heating equipment.

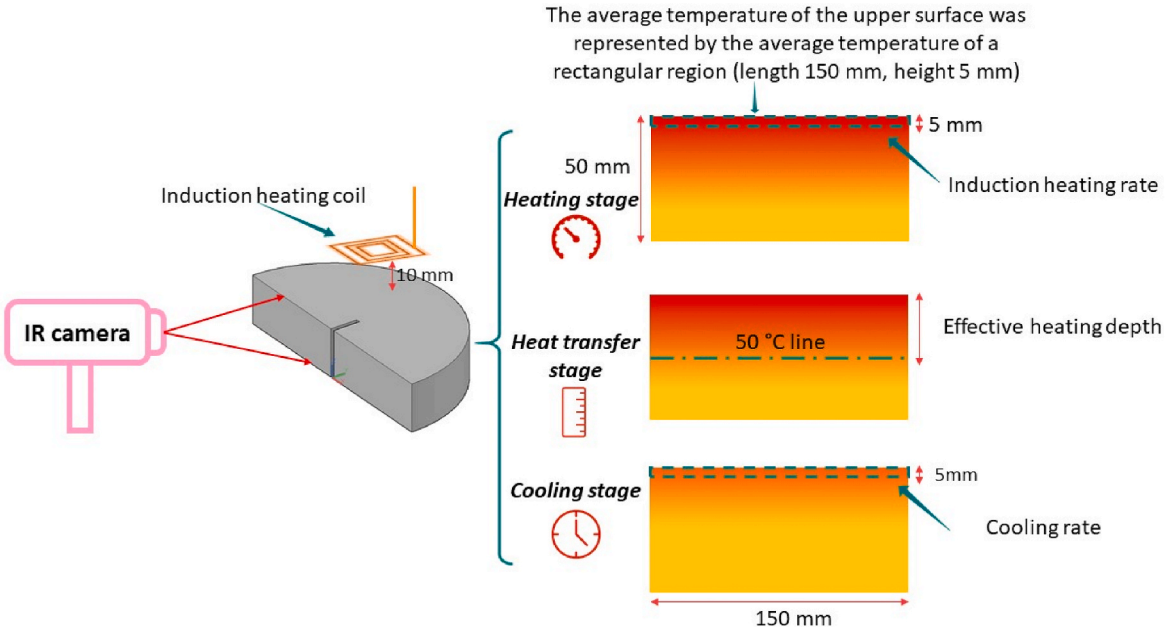

Fig. 4. Heating and temperature measurement method for SCB specimen.

the surface average temperature drops to 50 °C.

2.5. Multiple "fracture-healing" tests on asphalt mixture

As shown in Fig. 5, The multiple "fracture-healing" tests on SCB specimens were conducted to evaluate the multiple healing capability of asphalt mixture. The MTS-810 electronic universal testing machine was utilized to conduct the SCB test, which involved the following specific steps:

(1) Based on Fig. 5, the SCB specimens were placed in an environmental chamber at 25 °C for 6 h, and then the specimens were removed and installed on the support. The specimen was loaded at a rate of 50 mm/min, and vertical displacement and corresponding load values were recorded 100 times per second. To prevent excessive deformation of the specimen, the termination condition for loading was set as the load attenuating to 80% of the peak load.
(2) After the failure, the specimen was left to stand at 25 °C for 6 h, and then the sample was healed according to the heating method described in Section 2.4.
(3) As shown in Fig. 5,the healed samples were placed in a 25 °C environment for 24 h, and then the above steps were repeated until the healing rate reached the specified value.

The loading curve generated during the loading process is shown in Fig. 6, and the critical load value (P) can characterize the strength characteristics of the specimen. Fracture energy is a crucial metric that quantifies the energy dissipated by a specimen during the fracturing process, offering valuable insights into the fracture behavior of asphalt mixtures. In this study, the Fracture Energy Recovery Rate (FERR) serves as a pivotal parameter for assessing the self-healing performance of the asphalt mixture, as shown in Eq. (1) and Eq. (2). The effectiveness of FERR in evaluating self-healing performance lies in its capacity to capture the material's ability to recover from fractures. A higher FERR indicates a proficient healing process that can effectively restore fracture energy, thereby highlighting the material's enhanced resilience and durability across repeated loading cycles.

$$FERR_i = \frac{G_i}{G_0} = \frac{\frac{W_i}{\text{Area}}}{\frac{W_0}{\text{Area}}} = \frac{U_i}{U_0} \times 100\% \quad (1)$$

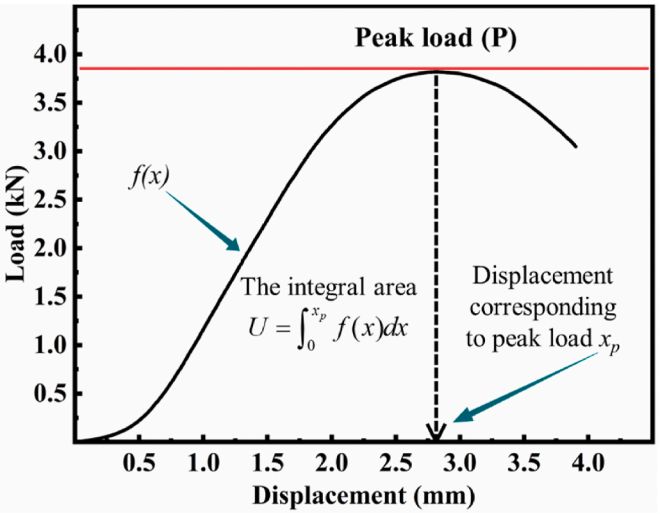

Fig. 6. SCB loading curve.

$$Area = (r - a)t \quad (2)$$

Where $FERR_i$ was defined as the ratio of fracture energy; G_i represented the fracture energy value for the i-th loading after the initial loading, J/m^2; G_0 represented the initial loading fracture energy value, J/m^2; W_i corresponded to the breaking work after the first cycle of loading, with the same size as the integral area, J; W_0 represented the fracture work for the first load, also with the same size as the integral area, J; *Area* referred to the connecting area in the middle of the sample, mm^2; *r* denoted the sample radius, mm; *a* represented the length of the incision, mm; t was the thickness of the sample, mm. It should be noted that $Area_i$ and $Area_0$ have the same size under the experimental conditions in this study.

3. Results and discussion

3.1. Viscosity and workability requirement of WCFMA

Fig. 7 shows the viscosity of the pen 70 and WCFMA at different temperatures. One evident trend observed was that the viscosity of asphalt binder exhibited a gradual increase with the augmentation of

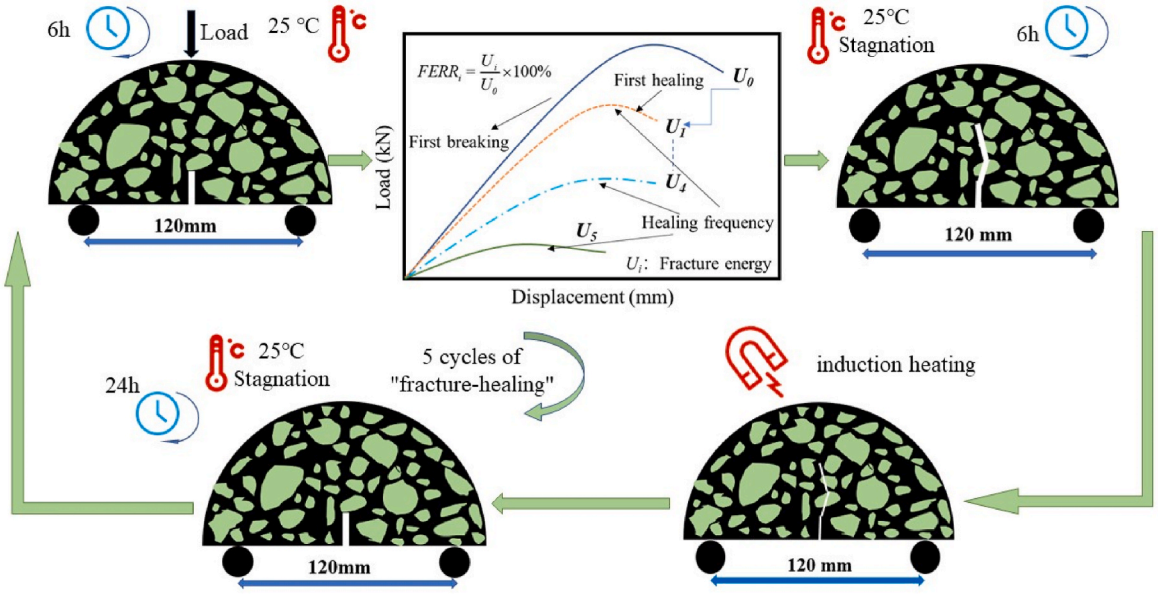

Fig. 5. Multiple "fracture-healing" tests scheme.

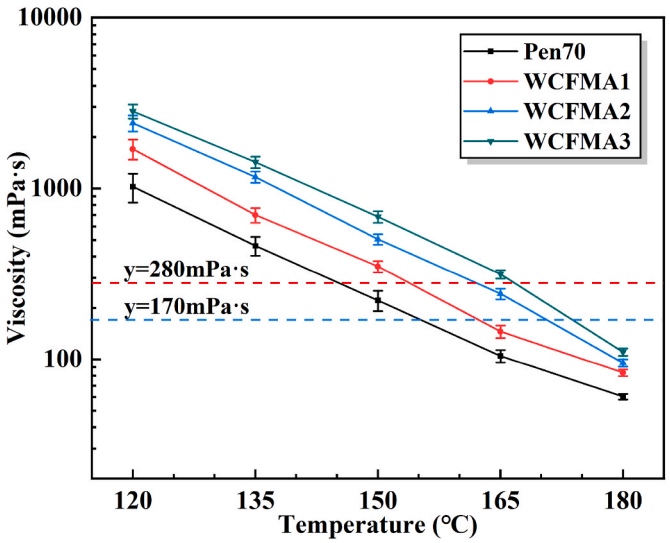

Fig. 7. Viscosity at different temperatures for Pen70 and WCFMA.

WCFs dosage, while it underwent a decrease with elevated temperatures. Specifically, at a consistent test temperature (using the example of viscosity at 150 °C), with every 1% increase in WCFs dosage, the viscosity of asphalt binder increased by 58.08%, 44.29%, and 35.45%, respectively. It was notable that as the dosage of WCFs increased, the rate of asphalt viscosity growth gradually diminished. This phenomenon could be attributed to the formation of a spatial network structure within the asphalt due to the higher WCFs dosage, thereby impeding the flow of lighter asphalt binder components (Yao et al., 2013). Consequently, the viscosity of the asphalt increased, leading to a deterioration in its workability during construction.

In order to ensure that the asphalt binder had reasonable workability during construction, the Superpave specifications recommended viscosities of approximately 170 mPa s and 280 mPa s for mixing and compaction of asphalt mixtures, respectively (JTG E20-2011). The corresponding mixing and compaction temperatures for asphalt binder at its optimal viscosity were determined based on the data presented in Fig. 7. Subsequently, the temperature data were presented in Fig. 8, facilitating a comprehensive understanding of the relationship between construction temperature and WCFs dosage. Upon analyzing Fig. 8, it

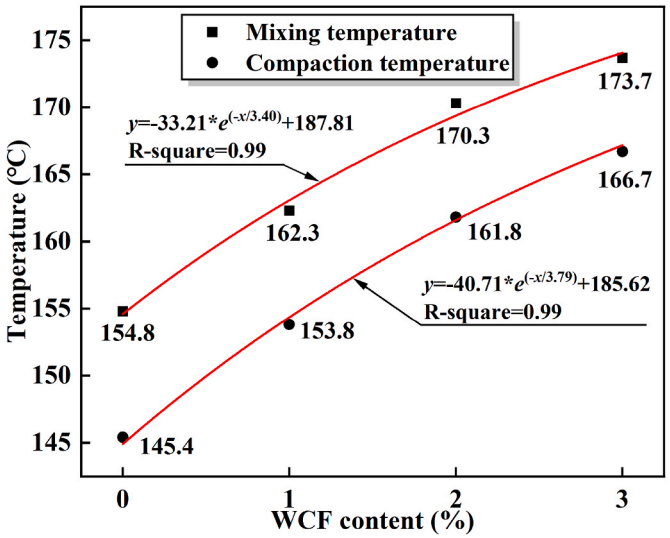

Fig. 8. Required temperatures of WCFMA with different dosages of WCFs for mixing and compaction of asphalt mixture.

became apparent that the optimal mixing temperatures for Pen70, WCFMA1, WCFMA2, and WCFMA3 were determined as 154.8 °C, 162.3 °C, 170.3 °C, and 173.7 °C, respectively. Furthermore, the optimal compaction temperatures for these asphalt types were determined as 145.4 °C, 153.8 °C, 161.8 °C, and 166.7 °C. Regression analysis yielded significant results, indicating a pronounced exponential relationship between the dosage of WCFs and the corresponding construction temperature.

The introduction of WCFs in asphalt binder required an increase in temperature to ensure proper workability, as depicted in Fig. 8. However, raising the temperature resulted in higher energy consumption, which contradicted the goals of cleaner production. In conclusion, the addition of WCFs enhanced the viscosity and road performance of asphalt to a certain degree. Nonetheless, an excessive content of WCFs will have adverse effects on the workability during construction and also impact the flowability of asphalt during the induction heating process. Therefore, it is crucial to maintain an appropriate dosage of WCFs to optimize their benefits. After comprehensive consideration, the dosage of WCFs was set at 1% by weight of the virgin asphalt binder.

3.2. Evaluation of temperature characteristics of asphalt mixture

3.2.1. Heating performance analysis

The induction heating rate directly determined the efficiency of induced healing in asphalt mixture. The variations of the average surface temperature over time for the three asphalt mixture specimens after induction heating were shown in Fig. 9. It was observed from Fig. 9 that, under the heating mode of 3 s of heating followed by 1 s of rest, the average surface temperature of the asphalt mixture specimens exhibited an overall upward trend. Specifically, the surface average temperatures of W2, P2, and P4 all reached 110 °C, requiring heating durations of 48 s, 59 s, and 30 s, respectively. The linear regression analysis of the temperature-time relationship yielded heating rates of 1.48 °C/s, 1.27 °C/s, and 2.51 °C/s for W2, P2, and P4, respectively. Compared to P2, the heating rates of W2 and P4 increased by 16.5% and 97.6%, respectively. It became evident that directly increasing the dosage of steel fibers proved more effective in enhancing the heating rate of asphalt mixture. Additionally, it was found that incorporating WCFs into the mixture, without altering the dosage of steel fibers, also contributed to an improvement in the induction heating rate of asphalt mixture to a certain extent.

To analyze the induction heating rate characteristics of asphalt mixture more accurately, the heating process was divided into four stages: Stage 1 (25–50 °C), Stage 2 (50–75 °C), Stage 3 (75–100 °C), and Stage 4 (100–125 °C). The time taken for each stage was recorded, and the results were presented in Fig. 10.

From Fig. 10, it can be observed that P2 required the longest heating time in each stage. On the other hand, compared to P2, P4 exhibited the shortest heating time in each stage. By increasing the dosage of steel fibers by 2%, the asphalt mixture generated more heat internally. The heating times for P4 in each stage were reduced by 62.5%, 37.5%, 50.0%, and 33.3%, respectively. The inclusion of WCFs significantly enhanced the heating rate of W2 in Stage 1, reducing the heating time by 50.0% compared to P2. However, in Stages 2–4, the heating times for P2 and W2 were essentially the same. This suggested that within the temperature range of 50–110 °C, the WCFs did not exhibit a substantial improvement in the heating and temperature rise performance of the asphalt mixture surface. One possible explanation for this phenomenon was that the addition of WCFs enhanced the ability of asphalt mixture to absorb heat in Stage 1, resulting in a rapid increase in the surface temperature of the specimens. However, as the heating time increased, the WCFs could not generate eddy currents and generate heat under the magnetic field, failing to provide additional heating sources for the asphalt mixture. Moreover, the average surface temperature could not reflect the gradient of heat transfer in the vertical direction. Therefore, the heating times for P2 and W2 were similar in the subsequent three

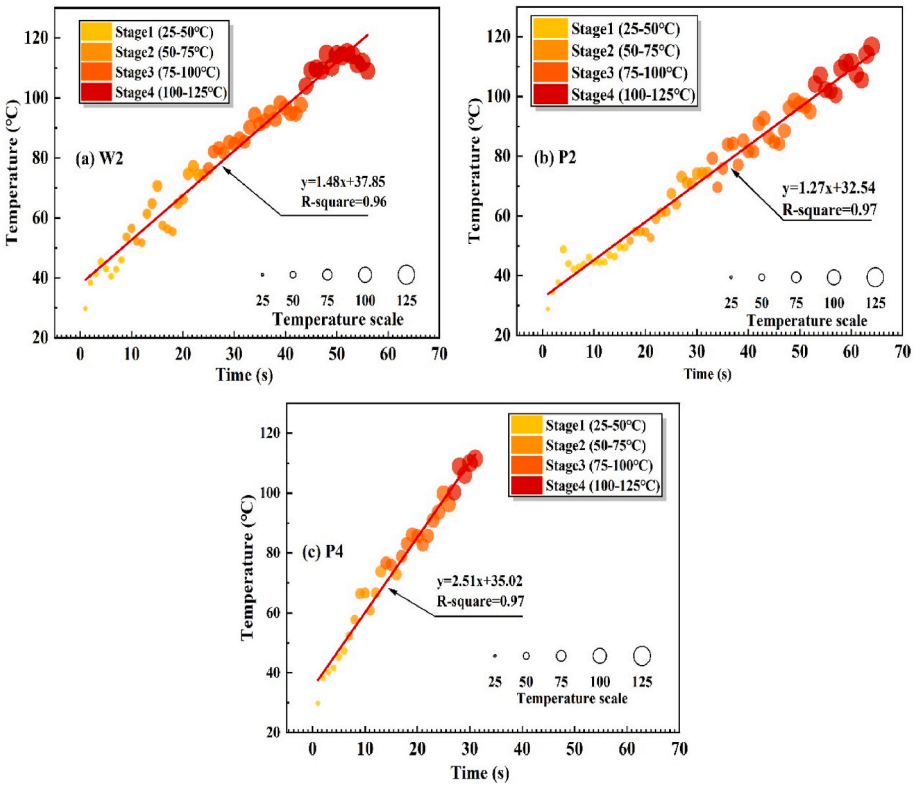

Fig. 9. Variation of the average surface temperature of asphalt mixture under induction heating: (a) W2: WCFMA1+2%wt steel fibers; (b) P2: Pen70 + 2%wt steel fibers; (c) P4: Pen70 + 4%wt steel fibers.

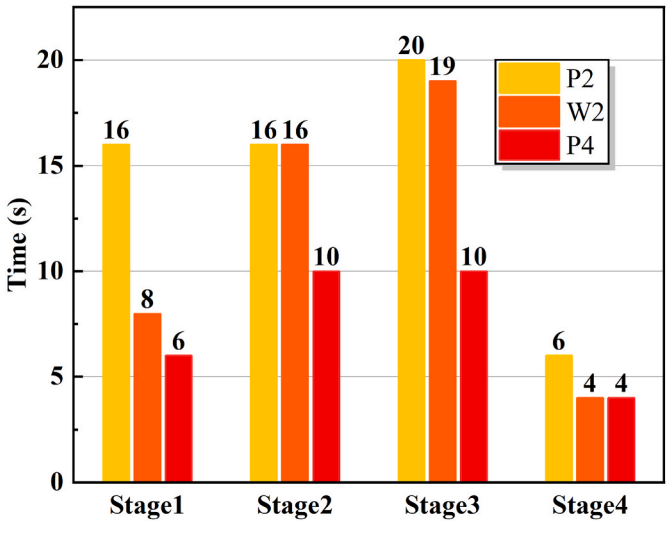

Fig. 10. The duration of different heating stages in asphalt mixture.

stages.

3.2.2. *Effective heating depth analysis*

The surface heating rate reflected the heating performance of asphalt mixture under induction heating, while the vertical heat conduction in asphalt mixture determined the effective heating depth. The infrared images of temperature conduction in the vertical direction of asphalt mixture after induction heating are shown in Fig. 11. The color difference in the infrared image could effectively reflect the variations in temperature conduction within the asphalt mixture specimens over time. In this context, brighter colors represented high-temperature areas, while darker colors represented low-temperature areas. According to the results of previous experiments, a minimum effective healing temperature of 50 °C was established for asphalt mixture. As shown in Fig. 11, the depth corresponding to a temperature of 50 °C in the vertical direction of the SCB specimen was measured using infrared analysis tools, and the rectangular area from the top of the specimen to the effective depth was defined as the effective heating area of the asphalt mixture.

From Fig. 11, it could be observed that the effective heating depths inside the three types of asphalt mixture varied over time. For W2, as time increased, the effective heating depth range continuously deepened, and by the 6th minute, the temperature throughout the entire specimen had reached the effective healing temperature, with an effective heating depth of 50 mm. For P2, within the first 2 min of heat transfer, the effective heating depth range continuously deepened. Between 2 and 4 min, the effective heating depth reduced, and during the 4 to 6-min process, the effective heating depth remained constant. For P4, within the first 2 min, the effective heating depth continuously deepened, while between 2 and 4 min, the effective heating depth remained constant. During the 4 to 6-min process, the effective heating depth decreased.

In order to further quantify the variations in effective heating depth inside the asphalt mixture specimens, the results of the effective heating depth within each specimen over time were presented in Fig. 12. In Fig. 12, the negative values of the effective heating depth stem from the selection of the specimen surface as the reference point. When examining depths below this reference point, the negative values inherently indicate positions relative to the surface. From the results in Fig. 12, it could be observed that only the effective heating depth of W2 gradually increased with time, achieving complete and effective heating of the 50 mm thick specimen within 6 min. At the 2 nd min, both P2 and P4 specimens reached their maximum effective heating depths, measuring 32.6 mm and 32.4 mm, respectively. The effective heating depths of P2 and P4 were approximately equal at this time, while the effective

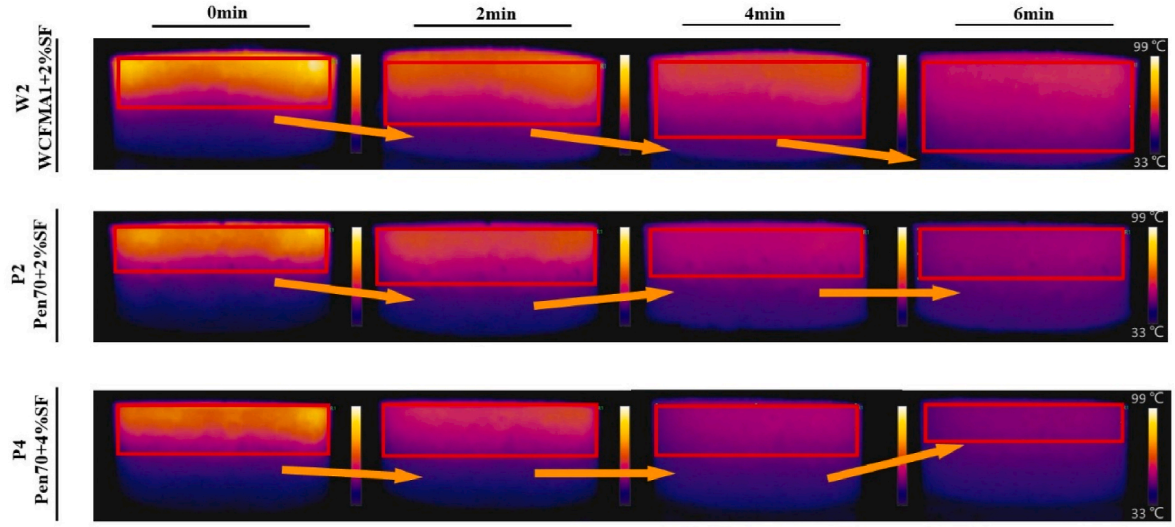

Fig. 11. Effective heating depth of different asphalt mixture after induction heating for different time.

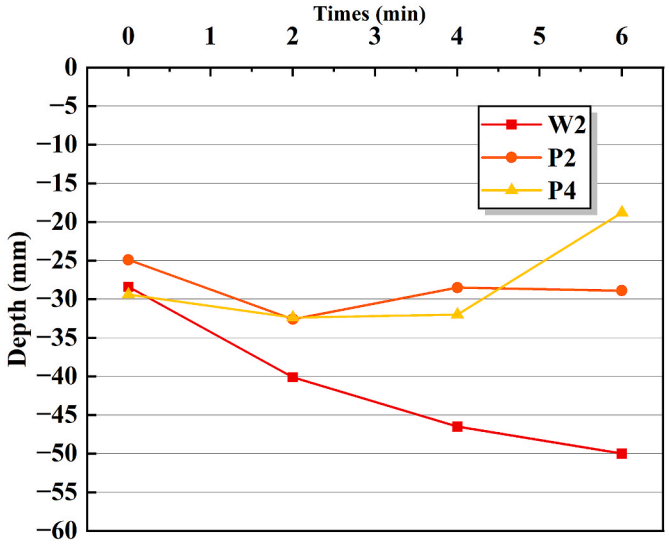

Fig. 12. Trend of effective heating depth of asphalt mixture with time.

heating depth of W2 was 40.1 mm, indicating an increase of approximately 7.5 mm compared to P2 and P4. This also indicated that WCFs could greatly promote the vertical heat transfer of steel fiber asphalt mixture, significantly increasing the effective depth of induction heating. This was because WCFs were flexible materials with excellent thermal conductivity and electrical conductivity. Through the modification of the virgin asphalt binder, they could be fully dispersed into the asphalt mixture. WCFs not only enhanced the heat absorption capacity of the asphalt mixture but also effectively transferred surface heat continuously to the interior of the asphalt mixture, thereby improving the uniformity of induction heating in asphalt mixture. This provided the possibility for induction heating of thicker asphalt pavements.

In addition, it was worth noting that although the average surface temperature rise rate of P4 was the highest, the effective heating depth did not increase compared to P2. Furthermore, after 4 min, the effective heating depth of P4 would decrease. This was due to the fact that while the heat performance of the steel fibers was strong, the increase in steel fiber content accelerated the heat exchange between the surface of the asphalt mixture and the surrounding environment, resulting in significant heat loss. This manifested as a decrease in the effective heating depth within the asphalt mixture specimens over time. Therefore, it is necessary to control the content of steel fibers within a reasonable range.

3.2.3. Cooling process characterization

After the cessation of heating, the time-dependent variations of average surface temperature for three types of asphalt mixture are shown in Fig. 13. According to the fitting results from Fig. 13, the average surface temperature of the asphalt mixture exhibited a single exponential decay trend as time elapsed. Among them, P4 had the fastest temperature decay, followed by P2, while W2 had the slowest average surface temperature decay. The time required for W2, P2, and P4 to reach a surface average temperature of 50 °C was 20 min, 12 min, and 8 min, respectively. This result also indicated that the addition of WCFs significantly prolonged the duration of asphalt mixture at the effective healing temperature.

Through a comparison between P2 and P4, coupled with the insights derived from the effective heating depth analysis in Section 3.2.2, it was concluded that W2 facilitated efficient heat conduction from the surface into the specimen's interior. This process minimized thermal radiation transfer between the specimen's surface and the surrounding environment, thereby reducing heat loss. Therefore, with the slowest cooling

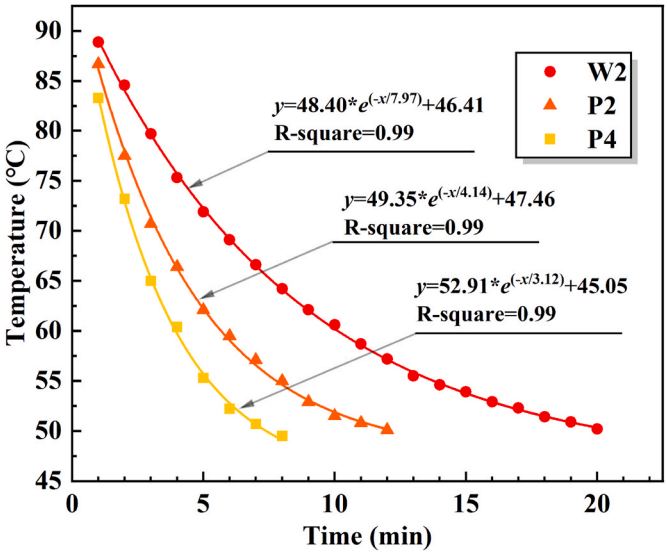

Fig. 13. Trend of average surface temperature changes in asphalt mixture over time post induction heating.

rate, W2 enabled heat to be distributed evenly within the asphalt mixture and to be maintained for a sustained period, effectively facilitating the self-healing process of the asphalt mixture. Additionally, the rapid decrease in surface temperature for P4 also fully explained the phenomenon of reduced effective heating depth in the latter half.

3.3. Analysis of multiple "fracture-healing" behavior of asphalt mixture

3.3.1. Variation patterns of mechanical strength

Through the utilization of SCB testing, the force-displacement response of distinct asphalt mixture subjected to multiple "fracture-healing" cycles was meticulously scrutinized. For the purpose of clarity

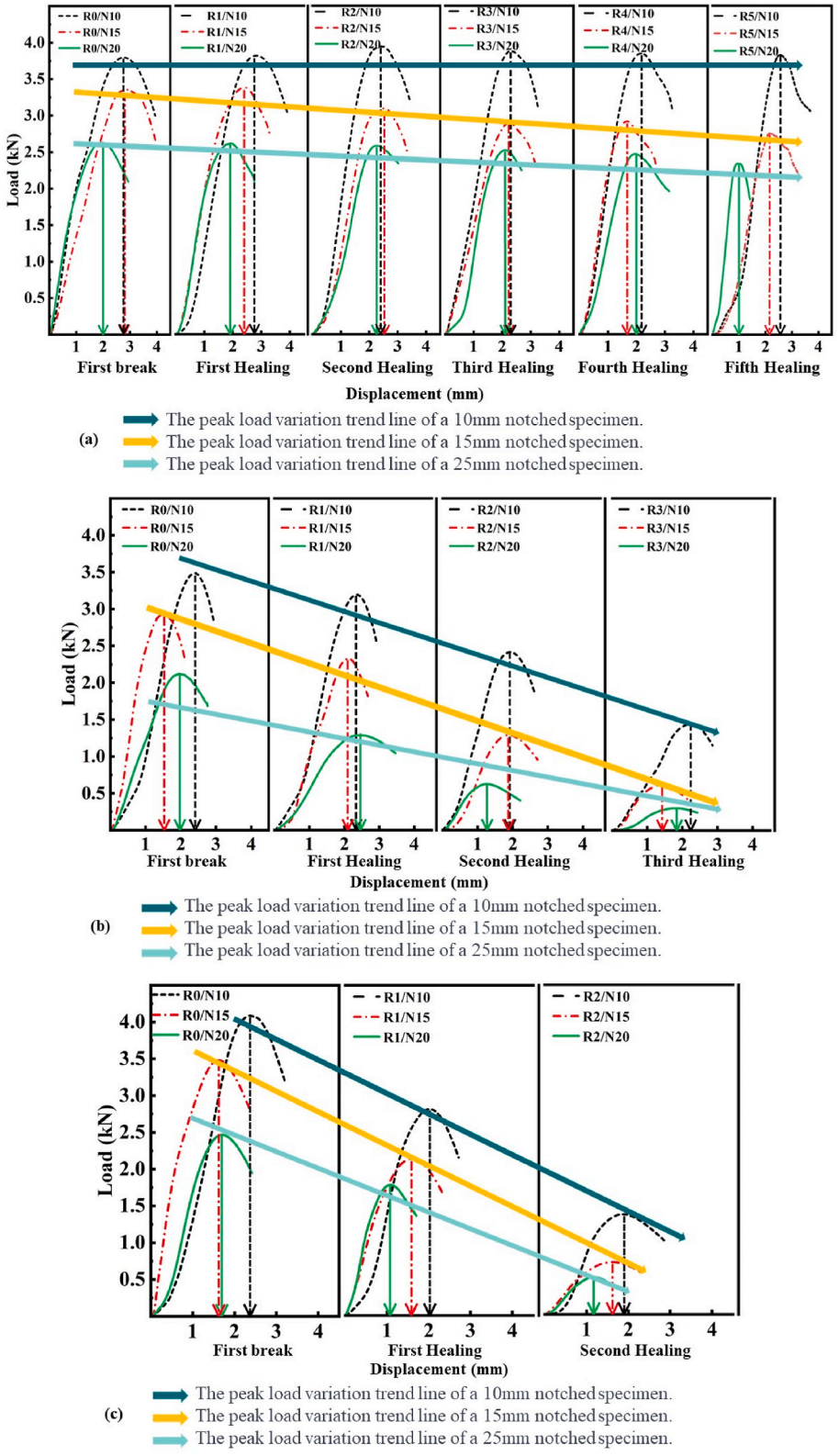

Fig. 14. Trends of force–displacement changes under cyclic fracture-healing: (a) W2; (b) P2; (c) P4.

expression, we shall employ the following notations: Let Rx denote the x-th healing process, while Ny shall represent the pre-existing notch length of the specimen as y.

As shown in Fig. 14, the loading curve of the first fracture indicated that for SCB specimens with the same crack depth, the peak load of W2 and P4 were similar, and both were higher than the peak load of P2. This suggested that when the steel fibers content in the asphalt mixture was 2%wt, increasing the steel fiber content or adding WCFs to the asphalt mixture enhanced its crack resistance. In fact, it had been proven that carbon fibers uniformly dispersed in asphalt mixture acted as reinforcements and improved its crack resistance (Wang et al., 2016). Compared to steel fibers, WCFs exhibited better stability and corrosion resistance at high temperatures and could be repeatedly used in induction heating. Additionally, WCFs had a higher elastic modulus and lower weight, which better prevented asphalt mixture from undergoing plastic deformation under loading, enhancing the stiffness and stability of mixture structures while reducing the load on the foundation and supporting structures (Akbar and Liew, 2020).

Moreover, significant differences were observed in the number of "fracture-healing" cycles that the three variations of asphalt mixture could endure. W2 proved capable of withstanding up to five "fracture-healing" cycles, whereas P2 and P4 could tolerate only three and two cycles, respectively. Notably, throughout these five cycles, the peak load of 10 mm notched SCB specimens from W2 showed minimal decrease and even exhibited a slight increase after the 2nd, 3rd, and 4th cycles. Conversely, the peak load of the 15 mm and 20 mm notched SCB specimens demonstrated a slight reduction as the number of cycles increased, suggesting that the asphalt mixture's strength in W2 recovered well after each healing cycle. In contrast, following 2–3 cycles, the peak load of SCB specimens from P2 and P4 fell dramatically, implying a less satisfactory strength recovery after multiple healing cycles for these asphalt mixture types.

3.3.2. Variation patterns of fracture energy

The recovery of SCB specimen strength provided insight into the wetting and filling effects of asphalt flow on cracks under the effective healing temperature. With an increasing number of "fracture-healing" cycles, stress damage accumulated gradually at the crack tip. Thus, it was imperative to analyze the healing process of asphalt mixture through an energy perspective.

By analyzing the loading curve, the fracture energy for SCB specimens with varied crack depths was calculated, as illustrated in Fig. 15. In addition, we closely examined and fitted the relationship between fracture energy and the number of healing cycles. As can be seen from Fig. 15, the deeper the crack depth in SCB specimens, the lower the required fracture energy. This phenomenon can be linked to the greater mechanical damage incurred from loading on deeper cracks, which facilitates easier failure of the specimens and consequently necessitates less fracture energy for failure.

Fig. 15 illustrates the fitting results for W2, showing a linear decrease in the fracture energy of the SCB specimen with increasing healing cycles, given a constant notch depth. After five healing cycles, the required fracture energies to cause a break in SCB specimens with notch depths of 10 mm, 15 mm, and 20 mm amounted to 62%, 46%, and 33% of the initial fracture energy, respectively. These findings support the concept that mechanical damage inflicted on the specimen by the crack increases in proportion with the notch depth. Moreover, with each successive "fracture-healing" cycle, stress damage at the crack site accumulated, leading to a pronounced decrease in the healing efficiency of the asphalt mixture. Therefore, to fully utilize the benefits of induction healing in asphalt pavements, it is crucial to perform induction heating healing early in the pavement's life. This approach can prevent stress damage accumulation under load, thereby achieving improved healing outcomes and effectively extending the pavement's service life. Fig. 15 (b) and **(c)** demonstrate similar trends for P2 and P4. Of note, the fitting results revealed that for the same notch depth, the fracture energy decay rate followed a descending order: P4 > P2 > W2. This rapid decay in fracture

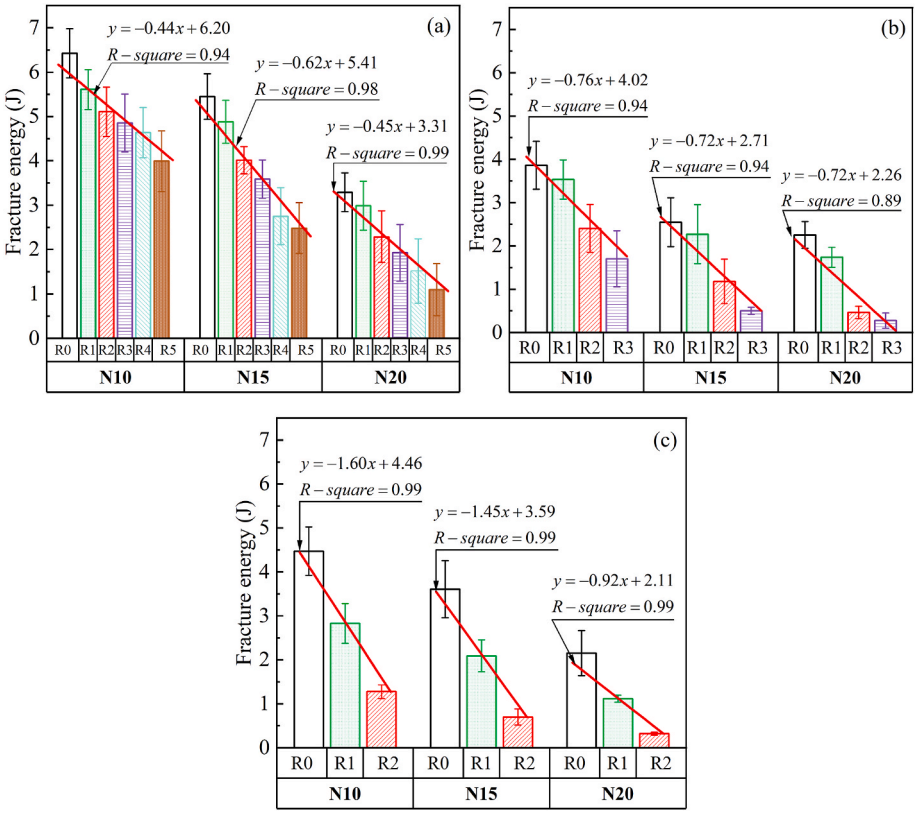

Fig. 15. Trends of fracture energy changes under cyclic "fracture-healing": (a) W2; (b) P2; (c) P4.

energy clearly indicated an inferior healing efficiency for P2 and P4.

3.3.3. Evaluation of multiple healing effect

Based on the results analysis in Sections 3.3.1 and 3.3.2, the Fracture Energy Recovery Rate (FERR) was selected as the healing indicator for asphalt mixture. The healing results for three types of asphalt mixture are displayed in Fig. 16.

Fig. 16 illustrates that the healing indicators for all three types of asphalt mixture decrease with the increasing number of "fracture-healing" cycles. The FERR provides a quantitative reflection of the stress damage accumulation in asphalt during multiple healing processes from an energy standpoint. This allows for a more accurate assessment of the healing condition of asphalt mixture. Notably, W2 managed to maintain a healing indicator of over 30% after undergoing five healing cycles - the highest among the three types. In contrast, P4 only managed two healing cycles, and the healing indicator dropped below 30% after the second cycle. P2, with a healing cycle limit of three, showed a FERR of only 21% for its 20 mm notched SCB specimen after the second healing, with the healing indicator dropping below 30%. These findings suggested that WCFs could improve the multiple healing potential of asphalt mixture, restore the strength of damaged asphalt mixture, and reduce stress damage accumulation during successive "fracture-healing" cycles. This underscored that when the steel fibers content exceeded 2%wt, an increase in steel fibers content could exacerbate the stress damage accumulation during "fracture-healing" cycles, significantly affecting the healing efficacy of asphalt mixture. In addition, these results also revealed that focusing solely on the surface heating rate when inducing asphalt mixture healing via induction heating could be limiting. To ensure optimal healing, it's essential to transfer the heat generated by electromagnetic induction fully into the asphalt mixture, increase the effective heating depth, and prolong the duration of the effective healing temperature.

3.4. Discussion on the mechanism of multiple "fracture-healing" of asphalt mixture

Fig. 17 illustrates the role of waste carbon fibers (WCFs) in enhancing the efficiency of multiple induction heating healing behaviors within asphalt mixture. The beneficial effects of WCFs on the asphalt mixture's capability for repeated "fracture-healing" can be attributed to two primary mechanisms.

Firstly, WCFs significantly enhance the vertical heat transfer efficiency within the asphalt mixture during induction heating. This heightened heat transfer efficiency ensures comprehensive self-healing initiation, even within 50 mm-thick SCB specimens. The extent of effective heating profoundly influences the realization of multiple heating healing effects.

Secondly, the incorporation of WCFs, combined with steel fibers, establishes a robust three-dimensional network structure within the asphalt mixture. This synergistic amalgamation of WCFs and steel fibers strengthens the material's resistance to cracks. Consequently, this arrangement leads to reduced mechanical damage during successive fracture occurrences, thereby minimizing cumulative mechanical degradation over multiple fracturing events. The reduction in the extent of this damage facilitates the rapid recovery of the strength and fracture energy of asphalt mixtures after induction heating.

Under these favorable conditions, characterized by complete and effective healing coupled with reduced mechanical damage, the strength and fracture energy of the W2 asphalt mixture undergo substantial rejuvenation. As a result, the number of healing cycles significantly increases, thereby vigorously promoting multiple induction heating healing behavior within the asphalt mixture.

4. Conclusions

This research offers innovative insights into enhancing asphalt

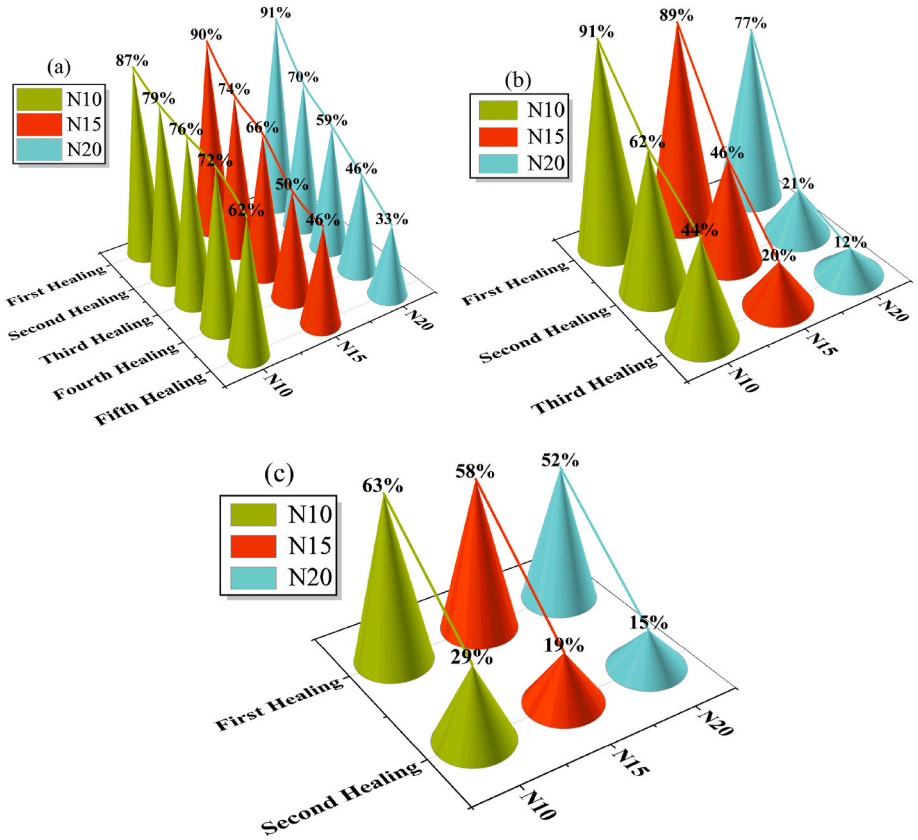

Fig. 16. Trends of FERR under cyclic "fracture-healing": (a) W2; (b) P2; (c) P4.

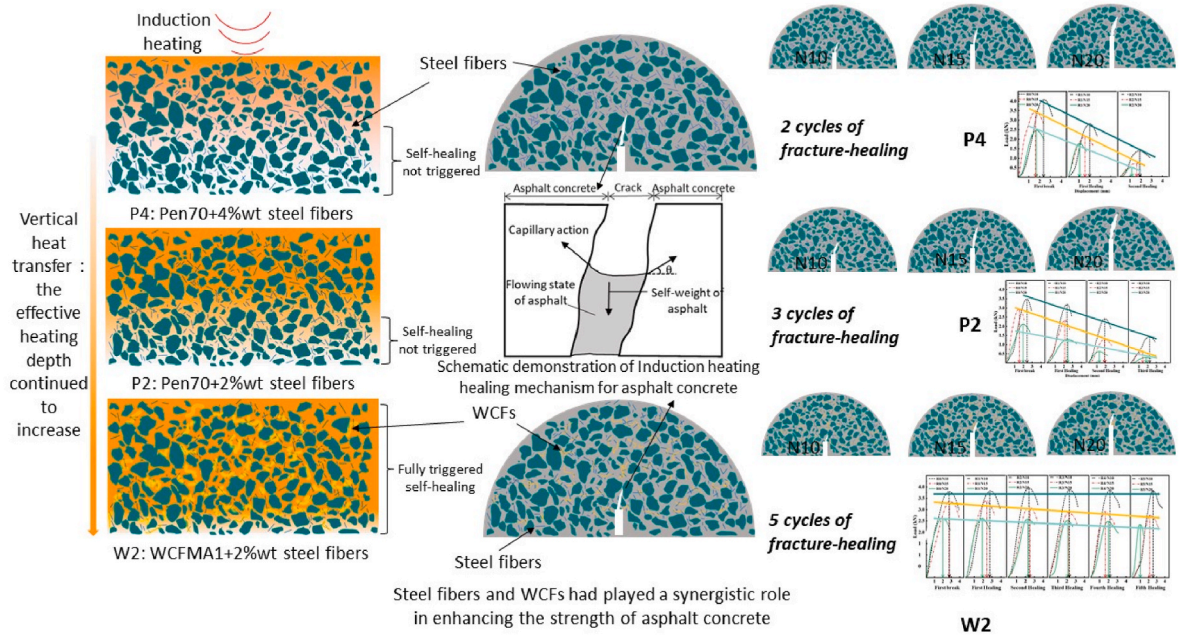

Fig. 17. Mechanism of waste carbon fibers on the efficiency of multiple induction heating healing behavior in asphalt mixture.

mixture self-healing using waste carbon fibers. while also promoting the resource recovery of waste carbon fibers in pavement engineering and more environmentally friendly road maintenance methods. Several critical conclusions can be summarized:

(1) WCFs were able to improve the viscosity of the virgin asphalt, but excessive WCFs content resulted in poorer workability of the asphalt binder. The optimal WCFs content was 1% (by weight of the virgin asphalt binder).
(2) WCFs slightly increased the induction heating rate of asphalt mixture, significantly improved the efficiency of heat transfer in the vertical direction within the asphalt mixture, and achieved effective heating of a 50 mm thick specimen within 6 min. In addition, WCFs slowed down the rate of decrease in the average surface temperature of asphalt mixture.
(3) WCFs enhanced the crack resistance of asphalt mixture during multiple "fracture-healing" cycles, and increased the number of "fracture-healing" cycles. At the same time, under the same number of cycles and destruction conditions, it enhanced the healing efficiency of the asphalt mixture.
(4) The mechanism by which WCFs promoted the effect of multiple induction healing of asphalt mixture was mainly explained in two aspects: on one hand, WCFs were able to reinforce the mixture, enhancing the crack resistance of asphalt mixture and reducing the accumulation of mechanical damage during multiple healing processes. On the other hand, the excellent thermal conductivity of WCFs enhanced the efficiency of heat transfer from the surface of asphalt mixture to the interior, effectively reducing heat loss, increasing the effective healing depth of asphalt mixture, extending the effective healing time, and providing more favorable conditions for the healing of cracks.

CRediT authorship contribution statement

Xiangqian Ye: Conceptualization, Methodology, Investigation, Experimental program, Writing – original draft. **Zhenyong Xiao:** Funding acquisition. **Chuang He:** Funding acquisition. **Wenyu Li:** Experimental program. **Peng Lin:** Conceptualization, Writing – review & editing. **Yuanyuan Meng:** Writing – review & editing. **Chichun Hu:** Supervision, Funding acquisition.

Declaration of competing interest

The authors declare that they have no known competing financial interests or personal relationships that could have appeared to influence the work reported in this paper.

Data availability

Data will be made available on request.

Acknowledgments

This research was supported by the Canton-Hong Kong Joint Research Program (2019A0503004), the Opening Project Fund of Materials Service Safety Assessment Facilities (MSAF-2021-006), and the Shanxi Provincial Department of Transportation Scientific Research Project (20-14K). Additionally, the work received support from the Science and Technology Project of Guangzhou Communications Investment Group Co. LTD and Guangzhou Expressway Management Co. LTD ((2021)-040).

References

Ajam, H., Gómez-Meijide, B., Artamendi, I., Garcia, A., 2018. Mechanical and healing properties of asphalt mixes reinforced with different types of waste and commercial metal particles. J. Clean. Prod. 192, 138–150.
Akbar, A., Liew, K., 2020. Assessing recycling potential of carbon fiber reinforced plastic waste in production of eco-efficient cement-based materials. J. Clean. Prod. 274.
Amani, S., Kavussi, A., Karimi, M.M., 2020. Effects of aging level on induced heating-healing properties of asphalt mixes. Construct. Build. Mater. 263.
Anupam, B., Sahoo, U.C., Chandrappa, A.K., 2022. A methodological review on self-healing asphalt pavements. Construct. Build. Mater. 321.
Ayar, P., Moreno-Navarro, F., Rubio-Gámez, M.C., 2016. The healing capability of asphalt pavements: a state of the art review. J. Clean. Prod. 113, 28–40.
Badroodi, S.K., Keymanesh, M.R., Shafabakhsh, G., 2020. Experimental investigation of the fatigue phenomenon in nano silica-modified warm mix asphalt containing recycled asphalt considering self-healing behavior. Construct. Build. Mater. 246.
Cao, X., Wang, H., Cao, X., Sun, W., Zhu, H., Tang, B., 2018. Investigation of rheological and chemical properties asphalt binder rejuvenated with waste vegetable oil. Construct. Build. Mater. 180, 455–463.
Cheng, H., Guo, L., Zheng, L., Qian, Z., Su, S., 2022. A closed-loop recycling process for carbon fiber-reinforced polymer waste using thermally activated oxide semiconductors: carbon fiber recycling, characterization and life cycle assessment. Waste Manage. (Tucson, Ariz.) 153, 283–292.

Fakhri, M., Bahmai, B.B., Javadi, S., Sharafi, M., 2020. An evaluation of the mechanical and self-healing properties of warm mix asphalt containing scrap metal additives. J. Clean. Prod. 253.
Garcia, A., Schlangen, E., Van De Ven, M., Van Vliet, D., 2011. Crack repair of asphalt concrete with induction energy. Heron 56 (1–2), 37–48.
Garcia, A., Salih, S., Gómez-Meijide, B., 2020. Optimum moment to heal cracks in asphalt roads by means electromagnetic induction. Construct. Build. Mater. 238.
Gómez-Meijide, B., Ajam, H., Lastra-González, P., Garcia, A., 2016. Effect of air voids content on asphalt self-healing via induction and infrared heating. Construct. Build. Mater. 126, 957–966.
Gómez-Meijide, B., Ajam, H., Garcia, A., Vansteenkiste, S., 2018. Effect of bitumen properties in the induction healing capacity of asphalt mixes. Construct. Build. Mater. 190, 131–139.
Gonzalez-Torre, I., Norambuena-Contreras, J., 2020. Recent advances on self-healing of bituminous materials by the action of encapsulated rejuvenators. Construct. Build. Mater. 258.
JTG E20-2011, 2011. Standard Test Methods of Bitumen and Bituminous Mixtures for Highway Engineering. Ministry of Transport of the People's Republic of China, Beijing.
JTG E42-2005, 2005. Testing Procedures of Aggregate for Highway Engineering in China. Ministry of Transport of the People's Republic of China, Beijing.
Karimi, M.M., Amani, S., Jahanbakhsh, H., Jahangiri, B., Alavi, A.H., 2021. Induced heating-healing of conductive asphalt concrete as a sustainable repairing technique: a review. Cleaner Engineering and Technology 4, 100188.
Khodaii, A., Khalifeh, V., Dehnad, M., Hamedi, G.H., 2014. Evaluating the effect of zycosoil on moisture damage of hot-mix asphalt using the surface energy method. J. Mater. Civ. Eng. 26 (2), 259–266.
Li, H., Yu, J., Wu, S., Liu, Q., Li, B., Li, Y., Wu, Y., 2019. Study on the gradient heating and healing behaviors of asphalt concrete induced by induction heating. Construct. Build. Mater. 208, 638–645.
Li, H., Schamel, E., Liebscher, M., Zhang, Y., Fan, Q., Schlachter, H., Köberle, T., Mechtcherine, V., Wehnert, G., Söthje, D., 2023. Recycled carbon fibers in cement-based composites: influence of epoxide matrix depolymerization degree on interfacial interactions. J. Clean. Prod. 411.
Liang, B., Lan, F., Shi, K., Qian, G., Liu, Z., Zheng, J., 2021. Review on the self-healing of asphalt materials: mechanism, affecting factors, assessments and improvements. Construct. Build. Mater. 266.
Liu, Q., García, Á., Schlangen, E., van de Ven, M., 2011. Induction healing of asphalt mastic and porous asphalt concrete. Construct. Build. Mater. 25 (9), 3746–3752.
Liu, Q., Schlangen, E., van de Ven, M., 2013. Characterization of the material from the induction healing porous asphalt concrete trial section. Mater. Struct. 46, 831–839.
Liu, Z., Luo, S., Wang, Y., Chen, H., 2019. Induction heating and fatigue-damage induction healing of steel fiber–reinforced asphalt mixture. J. Mater. Civ. Eng. 31 (9), 1943–5533.
Liu, J., Zhang, T., Guo, H., Wang, Z., Wang, X., 2022. Evaluation of self-healing properties of asphalt mixture containing steel slag under microwave heating: mechanical, thermal transfer and voids microstructural characteristics. J. Clean. Prod. 342.
Loizos, A., Karlaftis, M.G., 2005. Prediction of pavement crack initiation from in-service pavements: a duration model approach. Transport. Res. Rec. 1940 (1), 38–42.
Mawat, H.Q., Ismael, M.Q., 2020. Assessment of moisture susceptibility for asphalt mixtures modified by carbon fibers. Civ. Eng, J.-Tehran 6 (2), 304–317.
Meng, Y., Hu, C., Tang, Y., Großegger, D., Qin, W., 2022. Investigation on the erosion mechanism of simulated salt conditions on bitumen. Construct. Build. Mater. 334.
Mirhosseini, S.F., Khabiri, M., Kavussi, A., Kamali, M.J., 2016. Applying surface free energy method for evaluation of moisture damage in asphalt mixtures containing date seed ash. Construct. Build. Mater. 125, 408–416.
Norouzi, A., Richard Kim, Y., 2017. Mechanistic evaluation of fatigue cracking in asphalt pavements. Int. J. Pavement Eng. 18 (6), 530–546.
Qin, W., Hu, C., Meng, Y., 2021. Research on rheological property of hydrochar based bio modified asphalt binder: a promising way to solve environmental problems caused by waste corn stalks. Construct. Build. Mater. 308.
Schuster, S.L., Borges de Almeida Júnior, P.O., Faccin, C., Bueno, L.D., de Souza Chaves, B., Vestena, P.M., Specht, L.P., da Silva Pereira, D., 2023. Construction quality impact in asphalt pavements cost: a framework based on air voids, linear viscoelastic and fatigue behaviour. Int. J. Pavement Eng. 24 (1).
Slebi-Acevedo, C.J., Lastra-González, P., Pascual-Muñoz, P., Castro-Fresno, D., 2019. Mechanical performance of fibers in hot mix asphalt: a review. Construct. Build. Mater. 200, 756–769.
Souza, F.V., Castro, L.S., 2012. Effect of temperature on the mechanical response of thermo-viscoelastic asphalt pavements. Construct. Build. Mater. 30, 574–582.
Sun, D., Sun, G., Zhu, X., Guarin, A., Li, B., Dai, Z., Ling, J., 2018. A comprehensive review on self-healing of asphalt materials: mechanism, model, characterization and enhancement. Adv. Colloid Interface Sci. 256, 65–93.
Tapper, R.J., Longana, M.L., Norton, A., Potter, K.D., Hamerton, I., 2020. An evaluation of life cycle assessment and its application to the closed-loop recycling of carbon fibre reinforced polymers. Composites, Part B 184.
Vila-Cortavitarte, M., Jato-Espino, D., Castro-Fresno, D., Calzada-Pérez, M.Á., 2018. Self-healing capacity of asphalt mixtures including by-products both as aggregates and heating inductors. Materials 11 (5).
Wan, P., Liu, Q., Wu, S., Zhao, Z., Chen, S., Zou, Y., Rao, W., Yu, X., 2021. A novel microwave induced oil release pattern of calcium alginate/nano-Fe3O4 composite capsules for asphalt self-healing. J. Clean. Prod. 297.
Wang, X., Zhong, Y., 2019. Reflective crack in semi-rigid base asphalt pavement under temperature-traffic coupled dynamics using XFEM. Construct. Build. Mater. 214, 280–289.
Wang, Z., Dai, Q., Porter, D., You, Z., 2016. Investigation of microwave healing performance of electrically conductive carbon fiber modified asphalt mixture beams. Construct. Build. Mater. 126, 1012–1019.
Xu, S., García, A., Su, J., Liu, Q., Tabaković, A., Schlangen, E., 2018. Self-healing asphalt review: from idea to practice. Adv. Mater. Interfac. 5 (17).
Yang, H., Ouyang, J., Jiang, Z., Ou, J., 2023. Effect of fiber reinforcement on self-healing ability of asphalt mixture induced by microwave heating. Construct. Build. Mater. 362.
Yao, H., You, Z., Li, L., Goh, S.W., Lee, C.H., Yap, Y.K., Shi, X., 2013. Rheological properties and chemical analysis of nanoclay and carbon microfiber modified asphalt with Fourier transform infrared spectroscopy. Construct. Build. Mater. 38, 327–337.
Zhang, L., Liu, Q., Li, H., Norambuena-Contreras, J., Wu, S., Bao, S., Shu, B., 2019. Synthesis and characterization of multi-cavity Ca-alginate capsules used for self-healing in asphalt mixtures. Construct. Build. Mater. 211, 298–307.
Zhu, H., Yuan, H., Liu, Y., Fan, S., Ding, Y., 2020. Evaluation of self-healing performance of asphalt concrete for macrocracks via microwave heating. J. Mater. Civ. Eng. 32 (9).